Structural characterization of the fusion core in syncytin, envelope protein of human endogenous retrovirus family W

Rui Gong [a], Xiaoxue Peng [a], Shuli Kang [a], Huixing Feng [a], Jianying Huang [b], Wentao Zhang [a], Donghai Lin [b], Po Tien [a,*], Gengfu Xiao [a,*]

[a] *State Key Laboratory of Virology, College of Life Sciences, Wuhan University, Wuhan, Hubei 430072, China*
[b] *Shanghai Institute of Meteria Medica, Shanghai Institutes for Biological Sciences, Chinese Academy of Sciences, Shanghai 201203, China*

Abstract

Syncytin is a captive retroviral envelope protein, possibly involved in the formation of the placental syncytiotrophoblast layer generated by trophoblast cell fusion at the maternal–fetal interface. We found that syncytin and type I viral envelope proteins shared similar structural profiling, especially in the regions of N- and C-terminal heptad repeats (NHR and CHR). We expressed the predicted regions of NHR (41 aa) and CHR (34 aa) in syncytin as a native single chain (named 2-helix protein) to characterize it. 2-helix protein exists as a trimer and is highly α-helix, thermo-stable, and denatured by low pH. NHR and CHR could form a protease-resistant complex. The complex structure built by the molecular docking demonstrated that NHR and CHR associated in an antiparallel manner. Overall, the 2-helix protein could form a thermo-stable coiled coil trimer. The fusion core structure of syncytin was first demonstrated in endogenous retrovirus. These results support the explanation how syncytin mediates cytotrophoblast cell fusion involved in placental morphogenesis.
© 2005 Elsevier Inc. All rights reserved.

Keywords: Syncytin; Fusion; Human endogenous retrovirus; Envelope protein; Heptad repeats; Trophoblast cell

The fusion of lipid bilayers is central to a number of diverse biological processes, such as fertilization, vesicle trafficking, muscle development, placental morphogenesis, and viral infection. To date, the most extensively studied of these events is the membrane fusion of enveloped viruses. The surface glycoproteins of enveloped viruses can mediate virus–cell fusion or cell–cell fusion, which leads to the formation of syncytium.

Syncytin gene is the envelope protein (Env) gene of human endogenous retrovirus family W (HERV-W) and is located at human chromosome 7 (7q21.2) [1–3]. It encodes a protein of 538 amino acid residues. Robust syncytin gene expression was observed in placenta [1,2,4]. Human placenta contains a specialized cell type called trophoblast cell. At early gestation stage, mononuclear cytotrophoblast cells facing the maternal deciduas differentiate then fuse into a continuous layer of multinucleated syncytiotrophoblast. The syncytiotrophoblast layer is responsible for many functions performed by the placenta including transport of oxygen, nutrients, immune tolerance, and hormone production [5]. The hormone such as human chorionic gonadotropin (hCG) can be used as an indicator of syncytiotrophoblast formation [6].

Further research found that BeWo (a human trophoblastic choriocarcinoma line)/COS cell fusion could be achieved when BeWo cells were first transfected with a syncytin expression vector [1]. The same phenomena were also observed in other cell lines [3,4]. Anti-syncytin

antiserum reduced cell fusion significantly (to $49 \pm 9\%$), indicating that syncytin is a major agent responsible for BeWo/COS cell fusion [1]. It was also reported that specific inhibition of syncytin expression in the primary cytotrophoblasts using antisense oligonucleotides reduced syncytium formation [7].

Based on these observations, syncytin, as an envelope protein of HERV-W, is strongly considered as a fusogen that takes part in placentation through mediating cytotrophoblast cell fusion. Interestingly, we found that syncytin and HIV-1 envelope glycoprotein (gp) 160 shared similar structural profiling. HIV-1 gp160, a typical type I viral envelope protein, is proteolytically cleaved into two subunits: a surface subunit (gp120, SU) which is responsible for recognizing and binding to specific receptors on the host cell and a transmembrane subunit (gp41, TM) which contains the fusion peptide (FP), N- and C-terminal heptad repeats (NHR and CHR, also called HR1 and HR2). NHR and CHR can interact with each other and form a six-stranded α-helical bundle consisting of an inner triple-stranded coiled-coil buttressed by three C-helices, which is the fusion core structure of gp41 and crucial for membrane fusion [8,9].

Previous studies on many other enveloped viruses, including influenza virus, Newcastle disease virus, measles virus, mumps virus, and Menangle virus [10–14], have shown that the transmembrane subunits of these viral envelope proteins share common structural features with the HIV-1 gp41. Recently, our studies on the NHR and CHR regions in S2 domain of SARS coronavirus (SARS-CoV) spike protein revealed that one peptide, CP-1, derived from the CHR region inhibited SARS-CoV infection in the micromolar range. CP-1 and NP-1, a peptide derived from the NHR region mixed in equimolar concentrations, formed a six-helix bundle, similar to the fusion core structure of HIV-1 gp41 [15].

In the present paper, we analyzed the fusion core structure of syncytin.

Materials and methods

Amino acids sequence analysis of syncytin. Alignment of HIV-1 gp160 (NCB Accession No. Q70626) and syncytin (NCB Accession No. NP_055405) was performed using ClustalX 1.8. Heptad repeats in syncytin were predicted through the Coiled-coil program in http://www.ch.embnet.org/software/COILS_form.html [16].

Gene construction. The two heptad repeat regions (NHR and CHR) in syncytin were described as Figs. 1B and C. For the native single chain NHR + CHR construction (named 2-helix protein), we amplified the region from amino acids 349 to 445 in syncytin from one individual genomic DNA (PCR primers: 5′ GCA GGA TCC AAA CTA TCT CAA GAA CTA AAT G 3′ and 5′ GAT CTC GAG TCA CAT CCA TTG GCT GAG GAG 3′) and cloned it into the BamHI/XhoI restriction sites of the GST fusion expression vector pGEX-6P-1 (Amersham Pharmacia Biotech), in which there is a rhinovirus 3C

protease cleavage site for the fusion protein (same as the commercial PreScission protease cleavage site). The positive plasmids were verified by direct DNA sequencing. The native single chain NHR + CHR gene sequence was identical to previously published sequences [1,2].

Protein expression and purification. Escherichia coli strain BL21(DE3) transformed with the recombinant pGEX-6P-1 plasmid contained 2-helix protein gene was grown at 37 °C in 2× YT to an optical density of 0.8–1.0 (OD_{590}). Then it was induced with 1 mM IPTG at 22 °C for 6 h. Bacterial cells were harvested and resuspended in PBS (10 mM sodium phosphate, 150 mM NaCl, pH 8.0). Triton X-100 was then added to a final concentration of 1% and the bacterial cells were lysed by sonication at 0 °C. Lysate was subsequently clarified by centrifugation at 18,000g for 30 min at 4 °C. The clarified supernatants were passed over glutathione–Sepharose 4B column (equalized by PBS). The GST fusion protein (named GST-2-helix protein)-bound column was washed by PBS over 10 column volumes and eluted with glutathione elution buffer (10 mM reduced glutathione, 50 mM Tris · Cl, pH 8.0) for 1 column volume. The GST fusion protein was then cleaved by GST-fusion rhinovirus 3C protease (provided by Drs. K. Hudson and J. Heath) at 5 °C for 16 h in the cleavage buffer (50 mM Tris · Cl, pH 7.0; 150 mM NaCl; 1 mM DTT; and 1 mM EDTA, pH 8.0). The free GST, non-cleaved GST-2-helix protein, and the GST-fusion rhinovirus 3C protease were removed by passing over the glutathione–Sepharose 4B column again. The 2-helix protein was further purified through Hiload 26/60 Superdex G75 column (Amersham Pharmacia Biotech) running on ÄKTAexplorer 100 chromatography system (Amersham Pharmacia Biotech). The purified 2-helix protein was concentrated to a proper concentration which was determined by the method of Bradford (Bio-Rad). Then the protein was stored at −70 °C for further analysis.

Size exclusion-FPLC (SE-FPLC) analysis. The mixture of the purified 2-helix protein, BSA (Roche), and lysozyme (Sigma) was loaded into the Hiload 26/60 Superdex G75 column running on ÄKTAexplorer 100 chromatography system to assess oligomer formation. PBS was selected as mobile phase. The fractions of the peaks were collected, concentrated, and run on Tris–Tricine SDS–PAGE.

Chemical cross-linking. The purified 2-helix protein was dialyzed against cross-linking buffer (50 mM Hepes, 100 mM NaCl, pH 8.3) and concentrated to about 0.8 mg/mL by ultrafiltration (10 kDa cutoff). Proteins were cross-linked with ethylene glycol bis-(succinimidylsuccinate) (EGS) (Sigma). The reactions were incubated for 1 h on ice at concentrations of 0, 0.01, 0.1, 0.5, and 1.0 mM EGS, and stopped by 50 mM Tris · Cl (pH 8.0). Cross-linked products were analyzed on Tris–Tricine SDS–PAGE.

Circular dichroism spectroscopy. The secondary structure of the 2-helix protein was determined by circular dichroism (CD) spectroscopy. The purified protein was dissolved in PBS at the final concentration of 0.22 mg/mL, and the CD spectra were recorded on a Jasco J-810 spectrophotometer (Jasco, Easton, MD). Wavelength spectra were recorded at 25 °C using a 0.1-cm path-length cuvette. Thermodynamic stability was measured at 222 nm by recording the CD signal in the temperature range of 25–90 °C. The results were analyzed by the K2D program to evaluate α-helix content in the 2-helix protein [17]. This program can be found in http://www.cryst.bbk.ac.uk/cdweb/html/home.html [18].

Proteinase treatment. The purified GST-2-helix and 2-helix proteins were subjected to trypsin digestion in the proportions: 1/10 ([wt/wt], trypsin/protein) for 1 h at 37 °C. All the products of digestion were examined on Tris–Tricine SDS–PAGE immediately. Potential trypsin cleavage sites were predicted by PeptideCutter (http://us.expasy.org/tools/).

Molecular modelling and docking. The sequence alignment showed that NHR and CHR of syncytin shared about 44% and 62% sequence similarities, respectively, with the corresponding N-peptide (N36) and C-peptide (C34) of HIV-1 gp160 (Fig. 1A). The X-ray crystal structure of the gp160 core structure (N36–C34 complex) (PDB 1AIK) was used

A

syncytin NHR	352 QELNGDMERVADSLVTLQDQLNSLAAVVLQNRRALDLLTAE 392
HIV-1 gp160 N36	- - - SGIVQQQNNLLRAIEAQQHLLQLTVWGIKQLQARIL- -
	.* ::: : * ::: * : * .* :: :

syncytin CHR	407 YVNQSGIVTEKVKEIRDRIQRRAEELRNTGPWGL 440
HIV-1 gp160 C34	WMEWDREINNYTSLIHSLIEESQNQQEKNEQELL
	::: . :•: •• *:• *:• :: •:• *

B

C

NHR

CHR

Fig. 1. Amino acid sequence analysis of syncytin. (A) Alignment of NHR and CHR in syncytin on the corresponding N36 and C34 in HIV-1 gp160. NHR and N36 had 44% sequence similarity; CHR and C34 had 62% sequence similarity. (B) Putative structural domains in syncytin. SU subunit, surface subunit; TM subunit, transmembrane subunit; SP, signal peptide; FP, fusion peptide; NHR, N-terminal heptad repeats; CHR, C-terminal heptad repeats; TMD, transmembrane domain; and CP, cytoplasmic domain. Two coiled-coil heptad repeat regions were identified by the likelihood calculated by the Coiled-coil program. The construction of NHR + CHR protein (2-helix protein) was also shown (349–445). (C) Helix wheel analysis of the predicted coiled-coil regions of NHR and CHR. The amino acid residues at positions "a" and "d" were predominantly hydrophobic or neutral, typical for heptad repeat.

to build a model. Homology model of each peptide was built by the automated software Modeller 6.2 [19]. The model with the lowest objective function of ten models was selected. The ZDOCK 2.3 program was employed to model the interaction between NHR and CHR of syncytin. The ZDOCK program can be found in http://zlab.bu.edu/rong/dock/index.shtml [20]. The resultant model was evaluated further for its stereochemical properties by PROCHECK software [21] and represented by VMD v1.8.2 [22].

Results and discussion

Syncytin and HIV-1 gp160 shared similar structural profiling

By sequence analysis and alignment, we found that syncytin and HIV-1 gp160 shared similar structural

profiling, especially in the core structure, which was crucial for membrane fusion. Alignments of the sequences of NHR and CHR in syncytin and those in HIV-1 gp160 revealed that they have high sequence similarities (44% and 62%, respectively, Fig. 1A).

The fusion peptide (FP) was located at the N-terminus of syncytin TM subunit and consisted of hydrophobic, glycine-rich residues, which was essential for the initial penetration of the target cell membrane in many enveloped viruses, e.g., HIV-1 [23,24]. The hydrophobic 4–3 heptad repeat (HR) regions located adjacently to the N- and C-terminal portions of syncytin TM subunit were named as NHR and CHR, respectively (Figs. 1B and C). In HIV-1 gp41, these two regions form a stable, α-helical trimer of antiparallel dimers (trimer-of-hairpins), also called six-helix bundle, which represents the fusion-active core structure [25,26]. We built a single chain NHR + CHR construct (named 2-helix protein) to test whether the 2-helix protein can represent the fusion-active core structure of syncytin.

2-Helix protein exists as a trimer

The purified 2-helix protein was analyzed in SE-FPLC and chemical cross-linking for estimation of its molecular mass. When the mixture of the purified 2-helix protein, BSA, and lysozyme was run on SE-FPLC, three peaks (named peaks 1, 2, and 3) were found (Fig. 2). The 2-helix protein (peak 2, 34.4 kDa) was eluted between two standard proteins: BSA (peak 1, 67 kDa) (inset in Fig. 2, lane 1) and lysozyme (peak 3, 14.4 kDa) (inset in Fig. 2, lane 3), while the Tris–Tricine

Fig. 3. Chemical crosslinking of 2-helix protein. Cross-linked products were separated on Tris–Tricine SDS–PAGE followed by Coomassie brilliant blue staining. Protein markers (kDa) are shown in lane 1. Lanes 2–6 represent 0, 0.01, 0.1, 0.5, and 1.0 mM concentration of ethylene glycol bis (succinimidyl succinate) (EGS) used, respectively. Arrows corresponding to monomer, dimer, and trimer are indicated. They demonstrate that the 2-helix protein existed as trimer.

SDS–PAGE indicated that the molecular mass of peak 2 is about 11 kDa, corresponding to the monomer mass of the purified 2-helix protein (inset in Fig. 2, lanes 2 and 5). It indicated that the 2-helix protein might form a trimer ($3 \times 11 = 33$, closer to 34.4 kDa).

In chemical cross-linking of the 2-helix protein, one could clearly find the monomer, dimer, and trimer on the gel (Fig. 3). Tetramer and larger polymers were not observed. The results of SE-FPLC and chemical cross-linking suggested that the 2-helix protein might exist as a trimer.

2-Helix protein is highly α-helix, thermo-stable, and denatured by low-pH

The CD spectra recorded on 2-helix protein showed that it had high α-helical content (about 60%) at 25 °C (Fig. 4A, ●). The α-helical structure was slightly disrupted as the temperature increases (Fig. 4B). We found the curve still presented as a typical α-helical structure at 90 °C (Fig. 4A, ○), indicating that it was stable and the melting temperature (T_m) was higher than 90 °C. These observations suggested that the 2-helix protein trimer is highly α-helix, thermo-stable, which were similar to the characteristics of the fusion core structure of other viral envelope proteins including HIV-1 gp160, influenza virus HA, Newcastle disease virus F protein, and mouse hepatitis virus strain A59 (MHV-A59) spike protein [26,10,11,27].

We also tested the conformational change of 2-helix protein by acid denaturing. The α-helical structure of the 2-helix protein was disrupted gradually as pH value decreased, appearing to be in a folded state at pH 8.0 and in an unfolded state at pH 3.0 (Fig. 4C). The "S" shaped curve displayed that this unfolding
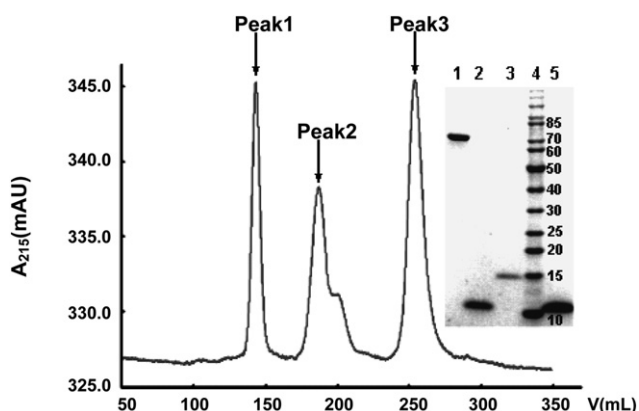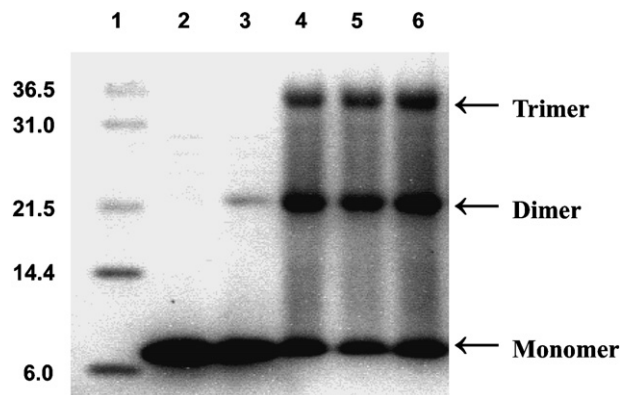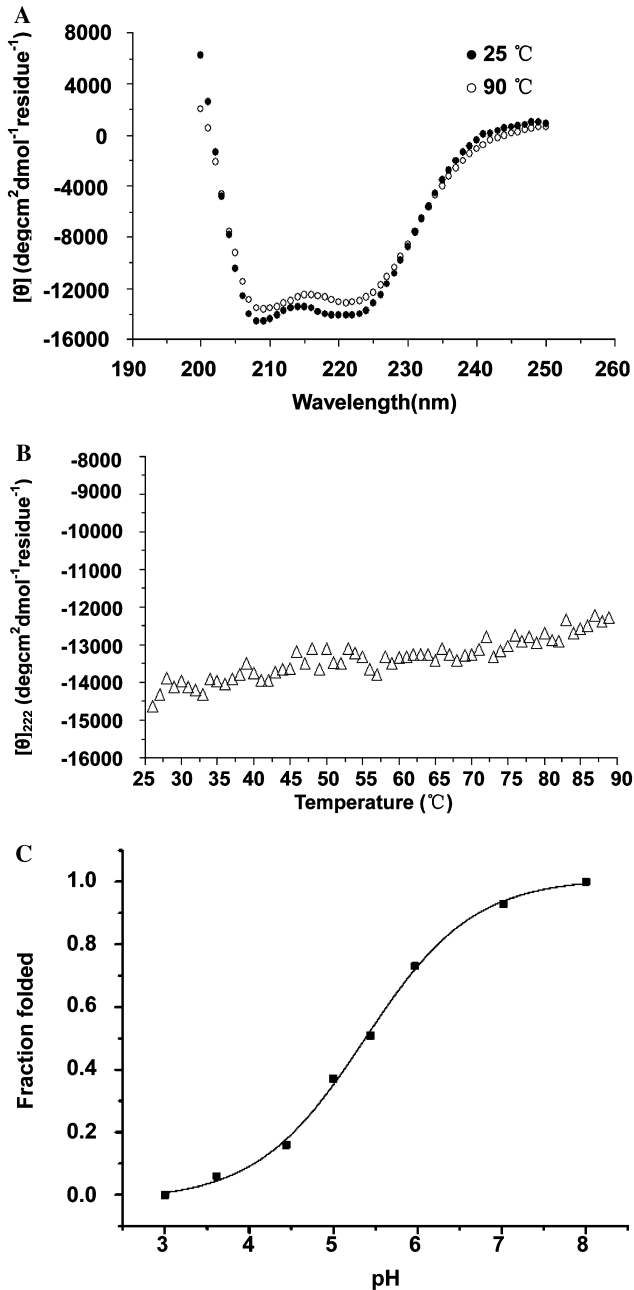

Fig. 2. SE-FPLC analysis of the 2-helix protein. The mixture of the 2-helix protein, BSA, and lysozyme was run on Superdex G75 gel-filtration. Inset was the Tris–Tricine SDS–PAGE result. Lanes 1, 2, and 3 are corresponding to the samples from the peaks 1, 2, and 3, respectively. Lane 4 is protein marker (kDa) and lane 5 is the purified 2-helix protein (11 kDa). The 2-helix protein (peak 2, 34.4 kDa) was eluted between BSA (peak 1, 67 kDa) and lysozyme (peak 3, 14.4 kDa) protein standards, which demonstrated that the 2-helix protein might form a trimer ($3 \times 11 = 33$ kDa, closer to 34.4 kDa).
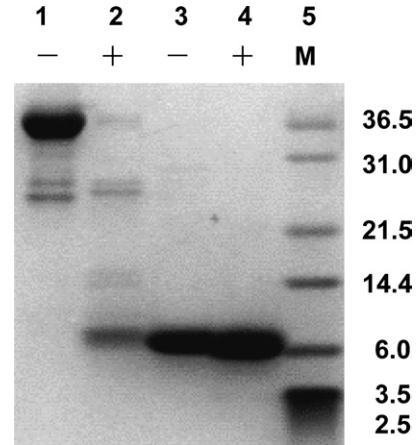
Fig. 5. Limited proteolysis of the 2-helix. Trypsin digestion: lanes 1 and 3 are the purified GST-2-helix and 2-helix protein without trypsin. Lanes 2 and 4 represent GST-2-helix and 2-helix protein digestion with trypsin in 1/10 ([wt/wt] trypsin/protein). Lane 5 is the protein marker (kDa).

HA, probably medicates cell fusion at neutral pH but not at low pH.

NHR and CHR could form a protease-resistant complex

We found that in the same trypsin concentration, the GST-2-helix protein was dramatically digested (Fig. 5, lane 2) while the 2-helix protein could hardly be digested (Fig. 5, lane 4), although there were the same proportions of trypsin digestion sites (total of digestion sites/total of amino acid residues) in the two proteins. There were 12 potential trypsin digestion sites in 2-helix protein. So if the structure of 2-helix protein was not compact enough, it ought to be digested to several fragments just as the digestion of GST-2-helix protein. But actually, 2-helix protein could hardly be digested, indicating that NHR and CHR in syncytin could form a protease-resistant complex.

Molecular modelling and docking of NHR and CHR in syncytin

Because the sequences of NHR and CHR in syncytin and those in HIV-1 gp160 had high sequence similarities (44% and 62%, respectively, Fig. 1A), a homology model of NHR–CHR complex could be built on the basis of the X-ray crystal structure of the HIV-1 gp41 core formed by the gp160 N36 and C34 [8,9]. Just like N36 and C34, both NHR and CHR in syncytin displayed putative coiled-coil structure (Fig. 6). The potential complex between NHR and CHR was then investigated by using the protein-docking software ZDOCK 2.3. The complex structure built by the docking technique demonstrated that NHR and CHR associated in an antiparallel manner (Fig. 6). Several hydrophobic interactions

Fig. 4. CD spectra of the 2-helix protein. (A) The 2-helix protein displayed typical α-helical secondary structures in 25 and 90 °C, with double minima of the ellipticities at 208 and 222 nm. (B) Thermal denaturing curves recorded at 222 nm from 25 to 90 °C with a scan rate of 1 °C/min. They illustrate that the 2-helix protein was thermostable. (C) Equilibrium isothermal unfolding of the 2-helix protein by acid denaturing. This experiment was performed at 25 °C. The fraction folded of the 2-helix protein (f_f) was calculated as $f_f = ([\theta] - [\theta_M])/([\theta_T] - [\theta_M])$. $[\theta_T]$ and $[\theta_M]$ were the mean residue ellipticities at 222 nm of the folded state at pH 8.0 and the unfolded states at pH 3.0, respectively.

course fitted a two-state model. A neutral condition was enough to make the structure of the 2-helix protein orderly and thermo-stable, which indicated that syncytin, like HIV-1 gp160 but not like influenza virus
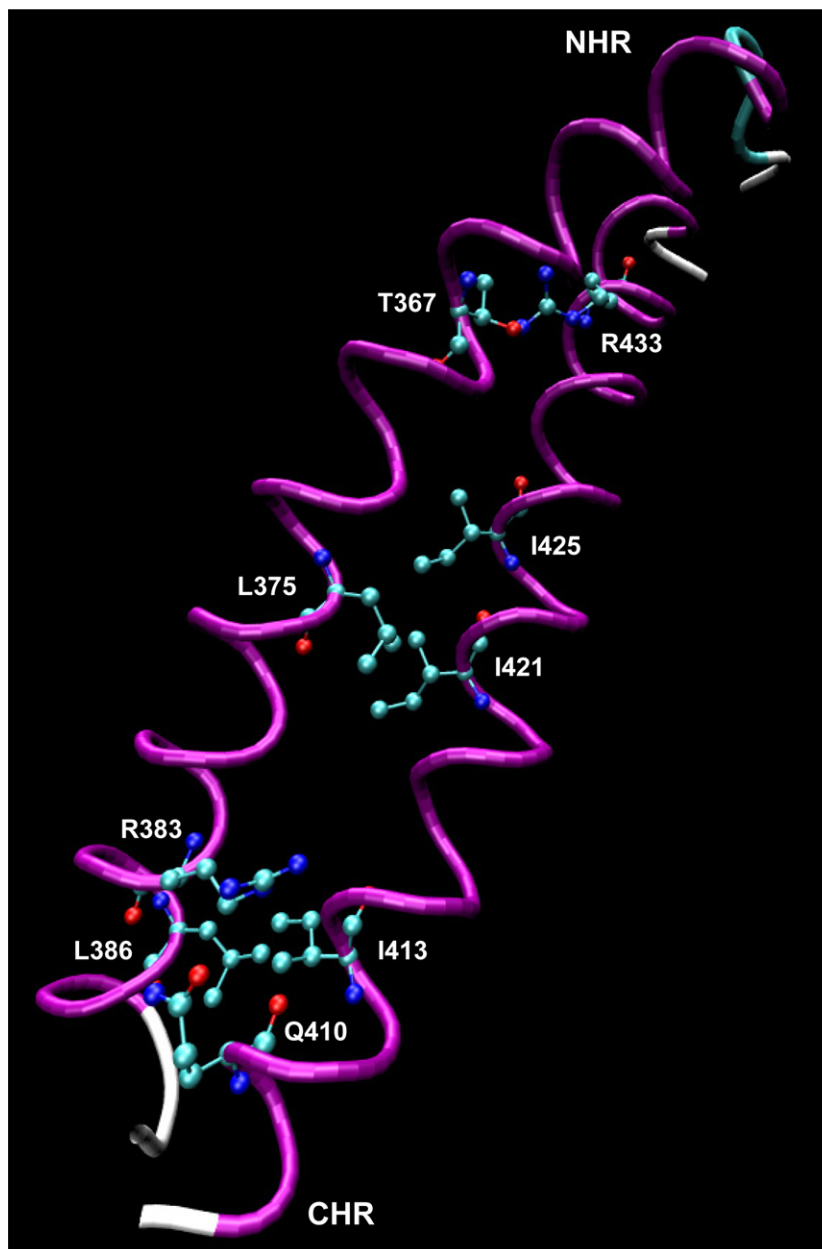
Fig. 6. Molecular modelling and docking. Molecular modelling indicated that both NHR and CHR in syncytin displayed putative coiled-coil structure. Interaction between NHR and CHR in syncytin was predicted by molecular docking. NHR and CHR associated in an antiparallel manner. L386 and L375 of NHR interacted with I413 and I421 of CHR, respectively, through hydrophobic interactions. T367 and R383 of NHR were hydrogen bonded to R433 and Q410 of CHR, respectively.

occurred between NHR and CHR, e.g., L386 and L375 of NHR interacted with I413 and I421 of CHR, respectively. There might be also several hydrogen bonds existing in the NHR–CHR complex, e.g., T367 and R383 of NHR were hydrogen bonded to R433 and Q410 of CHR, respectively. This model fitted well with an antiparallel dimer of NHR + CHR complex in syncytin, just like those in HIV-1 gp160 and coronavirus spike protein [8,9,27,28], and provided us putative detailed interactions between NHR and CHR in syncytin.

The fusion core structure in syncytin and implications for the fusion mechanism mediated by syncytin involved in placental morphogenesis

Several biophysical and biochemical methods were used to evaluate the structure of NHR+CHR (named 2-helix protein) in syncytin. Our experiments strongly implicated that the 2-helix protein in syncytin could form a stable triple-stranded coiled-coil, a structure commonly found in other type I viral envelope protein

fusion cores. Most retroviral envelopes have been shown to belong to the class I category of Env fusion proteins. We found syncytin also fitted the bill. The fusion core structure of syncytin is first demonstrated in endogenous retrovirus.

It might be reasonable to suggest that syncytin shares a common fusion mechanism with the type I viral envelope proteins. Previous and recent evidence suggest that the syncytin (HERV-W Env) is fusogenic and was directly involved in primary human trophoblast cell fusion and differentiation [1,3,4,7]. Basing on previous evidence and our results, the molecular fusion mechanism mediated by syncytin can be presumed as follows.

Syncytin SU subunit interacts with its corresponding cellular receptor: hASCT2 or hASCT1 [4,29]. Then, the TM subunit will change conformation to trigger the fusion processes. The TM subunit exposes and extends FP towards the target cell membrane using a "spring-loaded" model, which represents the feature of membrane fusion mediated by the influenza hemagglutinin HA$_2$ [30,31] and also to be adopted by other viral envelope proteins.

After FP punctures the cell membrane, syncytin NHR forms a homotrimeric coiled coil and then CHR surrounds this homotrimeric coiled coil to form a stable, α-helical trimer of antiparallel heterodimers (trimer-of-hairpins), or six-helix bundle. The fusion-active core structure brings the phospholipid bilayers in two cells into close proximity, resulting in membrane fusion and the formation of syncytiotrophoblast.

Syncytiotrophoblast formation derived from cytotrophoblast cell fusion is an important process in implantation and placentation. The above model provides some insights into the formation of syncytiotrophoblast caused by fusion events in detail. It is very similar to the syncytium formation during viral infection.

Recently, Chen's group reported that a peptide derived from CHR in syncytin was shown to potently inhibit syncytin-mediated cell fusion [32]. Their work in cell level is well complementary to our present studies in biophysical and biochemical aspects. Our results validate that NHR and CHR in the 2-helix protein form a thermo-stable coiled-coil trimer and also provide a possible explanation for this inhibition phenomenon: the peptides corresponding to the CHR region can inhibit fusion in a dominant-negative manner.

Acknowledgments

References

[1] S. Mi, X. Lee, X. Li, G.M. Veldman, H. Finnerty, L. Racie, E. LaVallie, X.Y. Tang, P. Edouard, S. Howes, J.C. Keith Jr., J.M. McCoy, Syncytin is a captive retroviral envelope protein involved in human placental morphogenesis, Nature 403 (2000) 785–789.

[2] J.L. Blond, F. Beseme, L. Duret, O. Bouton, F. Bedin, H. Perron, B. Mandrand, F. Mallet, Molecular characterization and placental expression of HERV-W, a new human endogenous retrovirus family, J. Virol. 73 (1999) 1175–1185.

[3] F. Mallet, O. Bouton, S. Prudhomme, V. Cheynet, G. Oriol, B. Bonnaud, G. Lucotte, L. Duret, B. Mandrand, The endogenous retroviral locus ERVWE1 is a bona fide gene involved in hominoid placental physiology, Proc. Natl. Acad. Sci. USA 101 (2004) 1731–1736.

[4] J.L. Blond, D. Lavillette, V. Cheynet, O. Bouton, G. Oriol, S. Chapel-Fernandes, B. Mandrand, F. Mallet, F.L. Cosset, An envelope glycoprotein of the human endogenous retrovirus HERV-W is expressed in the human placenta and fuses cells expressing the type D mammalian retrovirus receptor, J. Virol. 74 (2000) 3321–3329.

[5] K. Benirschke, P. Kaufmann, Pathology of the Human Placenta, fourth ed., Springer-Verlag, New York, 2000.

[6] J.L. Jameson, A.N. Hollenberg, Regulation of chorionic gonadotropin gene expression, Endocr. Rev. 14 (1993) 203–221.

[7] J.L. Frendo, D. Olivier, V. Cheynet, J.L. Blond, O. Bouton, M. Vidaud, M. Rabreau, D. Evain-Brion, F. Mallet, Direct involvement of HERV-W Env glycoprotein in human trophoblast cell fusion and differentiation, Mol. Cell. Biol. 23 (2003) 3566–3574.

[8] W. Weissenhorn, A. Dessen, S.C. Harrison, J.J. Skehel, D.C. Wiley, Atomic structure of the ectodomain from HIV-1 gp41, Nature 387 (1997) 426–430.

[9] D.C. Chan, D. Fass, J.M. Berger, P.S. Kim, Core structure of gp41 from the HIV envelope glycoprotein, Cell 89 (1997) 263–273.

[10] J. Chen, S.A. Wharton, W. Weissenhorn, L.J. Calder, F.M. Hughson, J.J. Skehel, D.C. Wiley, A soluble domain of the membrane-anchoring chain of influenza virus hemagglutinin (HA$_2$) folds in Escherichia coli into the low-pH-induced conformation, Proc. Natl. Acad. Sci. USA 92 (1995) 12205–12209.

[11] J. Zhu, P. Li, T. Wu, F. Gao, Y. Ding, C. Zhang, Z. Rao, G.F. Gao, P. Tien, Design and analysis of post-fusion 6-helix bundle of heptad repeat regions from Newcastle disease virus F protein, Protein Eng. 16 (2003) 373–379.

[12] J. Zhu, C. Zhang, Y. Qi, P. Tien, G.F. Gao, The fusion protein core of measles virus forms stable coiled-coil trimer, Biochem. Biophys. Res. Commun. 299 (2002) 897–902.

[13] Y. Liu, J. Zhu, M.G. Feng, P. Tien, G.F. Gao, Six-helix bundle assembly and analysis of the central core of mumps virus fusion protein, Arch. Biochem. Biophys. 421 (2004) 143–148.

[14] J. Zhu, C. Zhang, Z. Rao, P. Tien, G.F. Gao, Biochemical and biophysical analysis of heptad repeat regions from the fusion protein of Menangle virus, a newly emergent paramyxovirus, Arch. Virol. 148 (2003) 1301–1316.

[15] S. Liu, G. Xiao, Y. Chen, Y. He, J. Niu, C.R. Escalante, H. Xiong, J. Farmar, A.K. Debnath, P. Tien, S. Jiang, Interaction between heptad repeat 1 and 2 regions in spike protein of SARS-associated coronavirus: implication for virus fusogenic mechanism and identification of fusion inhibitors, Lancet 363 (2004) 938–947.

[16] A. Lupas, M. Van Dyke, J. Stock, Predicting coiled coils from protein sequences, Science 252 (1991) 1162–1164.

[17] M.A. Andrade, P. Chacon, J.J. Merelo, F. Moran, Evaluation of secondary structure of proteins from UV circular dichroism

spectra using an unsupervised learning neural network, Protein Eng. 6 (1993) 383–390.

[18] A. Lobley, L. Whitmore, B.A. Wallace, DICHROWEB: an interactive website for the analysis of protein secondary structure from circular dichroism spectra, Bioinformatics 18 (2002) 211–212.

[19] A. Sali, T.L. Blundell, Comparative protein modelling by satisfaction of spatial restraints, J. Mol. Biol. 234 (1993) 779–815.

[20] R. Chen, L. Li, Z. Weng, ZDOCK: an initial-stage protein-docking algorithm, Proteins 52 (2003) 80–87.

[21] R.A. Laskowski, D.S. Moss, J.M. Thornton, Main-chain bond lengths and bond angles in protein structures, J. Mol. Biol. 231 (1993) 1049–1067.

[22] W. Humphrey, A. Dalke, K. Schulten, VMD: visual molecular dynamics, J. Mol. Graph. 14 (1996) 33–38, 27–28.

[23] E.O. Freed, E.L. Delwart, G.L. Buchschacher Jr., A.T. Panganiban, A mutation in the human immunodeficiency virus type 1 transmembrane glycoprotein gp41 dominantly interferes with fusion and infectivity, Proc. Natl. Acad. Sci. USA 89 (1992) 70–74.

[24] H. Schaal, M. Klein, P. Gehrmann, O. Adams, A. Scheid, Requirement of N-terminal amino acid residues of gp41 for human immunodeficiency virus type 1-mediated cell fusion, J. Virol. 69 (1995) 3308–3314.

[25] M. Lu, S.C. Blacklow, P.S. Kim, A trimeric structural domain of the HIV-1 transmembrane glycoprotein, Nat. Struct. Biol. 2 (1995) 1075–1082.

[26] W. Weissenhorn, S.A. Wharton, L.J. Calder, P.L. Earl, B. Moss, E. Aliprandis, J.J. Skehel, D.C. Wiley, The ectodomain of HIV-1 env subunit gp41 forms a soluble, alpha-helical, rod-like oligomer in the absence of gp120 and the N-terminal fusion peptide, EMBO J. 15 (1996) 1507–1514.

[27] B.J. Bosch, R. van der Zee, C.A. de Haan, P.J. Rottier, The coronavirus spike protein is a class I virus fusion protein: structural and functional characterization of the fusion core complex, J. Virol. 77 (2003) 8801–8811.

[28] P. Ingallinella, E. Bianchi, M. Finotto, G. Cantoni, D.M. Eckert, V.M. Supekar, C. Bruckmann, A. Carfi, A. Pessi, Structural characterization of the fusion-active complex of severe acute respiratory syndrome (SARS) coronavirus, Proc. Natl. Acad. Sci. USA 101 (2004) 8709–8714.

[29] D. Lavillette, M. Marin, A. Ruggieri, F. Mallet, F.L. Cosset, D. Kabat, The envelope glycoprotein of human endogenous retrovirus type W uses a divergent family of amino acid transporters/cell surface receptors, J. Virol. 76 (2002) 6442–6452.

[30] C.M. Carr, P.S. Kim, A spring-loaded mechanism for the conformational change of influenza hemagglutinin, Cell 73 (1993) 823–832.

[31] P.A. Bullough, F.M. Hughson, J.J. Skehel, D.C. Wiley, Structure of influenza haemagglutinin at the pH of membrane fusion, Nature 371 (1994) 37–43.

[32] C. Chang, P.T. Chen, G.D. Chang, C.J. Huang, H. Chen, Functional characterization of the placental fusogenic membrane protein syncytin, Biol. Reprod. 71 (2004) 1956–1962.